



Calhoun: The NPS Institutional Archive
DSpace Repository

Faculty and Researchers

Faculty and Researchers Collection

2002

Determination of model valid prediction period using the backward Fokker-Planck equation

Chu, Peter C.; Ivanov, L.M.; Fan, C.W.

Chu, P.C., L.M. Ivanov, and C.W. Fan, 2002: Determination of model valid prediction period using the backward Fokker-Planck equation. Sixteenth Conference on Probability and Statistics in the Atmospheric Sciences, American Meteorological Society, 70-77

<http://hdl.handle.net/10945/36299>

Downloaded from NPS Archive: Calhoun



Calhoun is a project of the Dudley Knox Library at NPS, furthering the precepts and goals of open government and government transparency. All information contained herein has been approved for release by the NPS Public Affairs Officer.

Dudley Knox Library / Naval Postgraduate School
411 Dyer Road / 1 University Circle
Monterey, California USA 93943

<http://www.nps.edu/library>

2.4 DETERMINATION OF MODEL VALID PREDICTION PERIOD USING THE BACKWARD FOKKER-PLANCK EQUATION

Peter C. Chu, Leonid M. Ivanov, and C.W. Fan
Department of Oceanography
Naval Postgraduate School
Monterey, California

1. INTRODUCTION

A practical question is commonly asked: How long is an ocean (or atmospheric) model valid since being integrated from its initial state? Or what is the model valid prediction period (VPP)? To answer this question, uncertainty in ocean (or atmospheric) models should be investigated. It is widely recognized that the uncertainty can be traced back to three factors [Lorenz, 1963; 1984]: (a) measurement errors, (b) model errors such as discretization and uncertain model parameters, and (c) chaotic dynamics. The measurement errors cause uncertainty in initial and/or boundary conditions. The discretization causes small-scale "subgrid" processes to be either discarded or parameterized. The chaotic dynamics may trigger a subsequent amplification of small errors through a complex response.

The three factors are related to each other causing model uncertainty. Chu [1999] pointed out that the boundary errors act as a forcing term (stochastic forcing) in the Lorenz system. This suggests that the oceanic (or atmospheric) variables are sensitive to measurement errors (uncertain initial and/or boundary conditions), model errors (discretization), and chaotic (or stochastic) dynamics.

Currently, some time scale (e.g., e-folding scale) is computed from the instantaneous error (IE) growth to represent the model VPP. The faster the IE grows, the shorter the e-folding scale is, and in turn the shorter the VPP is. Using IE, evaluation of deterministic models becomes stability analysis in terms of either the leading (largest) Lyapunov exponent [e.g., Lorenz, 1969] or the amplification factors calculated from the leading singular vectors [e.g., Farrell and Ioannou, 1996 a, b]. For stochastic model, the statistical analysis becomes useful [Ehrendorfer, 1994 a, b;

Nicolis, 1992]. The probabilistic properties of the prediction error are described using the probability density function (PDF) satisfying the Liouville equation or the Fokker-Planck equation. Solving this equation, the mean and variance of errors can be obtained. Nicolis [1992] investigated the properties of error-growth using a simple low-order model (projection of Lorenz system into most unstable manifold) with stochastic forcing. A large number of numerical experiments were performed to assess the relative importance of average and random elements in error growth.

In fact, the IE growth rate is not the only factor to determine VPP. Other factors, such as the initial error and tolerance level of prediction, should also be considered. The tolerance level of prediction is defined as the maximum error the model can afford (still keeping the meaningful prediction). For the same IE growth rate, the higher the tolerance level (initial error) the longer (shorter) the model VPP is. Thus, the model VPP should be defined as the time period when the model error first exceeds a pre-determined criterion (i.e., the tolerance level ϵ). The longer the VPP, the higher the model predictability will be. In this study, we develop a theoretical framework of model predictability evaluation using VPP, and illustrate the usefulness and special features of VPP. The outline of this paper is depicted as follows. Description of prediction error of deterministic and stochastic models is given in Section 2. Estimate of VPP is given in Section 3. In Section 4, determination of VPP for a one-dimensional stochastic dynamic system is discussed. In Section 5, the conclusions are presented.

2. Prediction Error

2.1. Dynamic Law

Let $\mathbf{x}(t) = [x^{(1)}(t), x^{(2)}(t), \dots, x^{(n)}(t)]$ be the full set of variables characterizing the dynamics of the ocean (or atmosphere) in a

certain level of description. Let the dynamic law be given by

$$\frac{d\mathbf{x}}{dt} = \mathbf{f}(\mathbf{x}, t) \quad (1)$$

where \mathbf{f} is a functional. Deterministic (oceanic or atmospheric) prediction is to find the solution of (1) with an initial condition

$$\mathbf{x}(t_0) = \mathbf{x}_0 \quad (2)$$

where \mathbf{x}_0 is an initial value of \mathbf{x} .

With a linear stochastic forcing, $q(t)\mathbf{x}$, Eq.(1) becomes

$$\frac{d\mathbf{x}}{dt} = \mathbf{f}(\mathbf{x}, t) + q(t)\mathbf{x} \quad (3)$$

Here, $q(t)$ is assumed to be a random variable with zero mean

$$\langle q(t) \rangle = 0 \quad (4)$$

and pulse-type variance

$$\langle q(t) q(t') \rangle = q^2 \delta(t - t') \quad (5)$$

where the bracket $\langle \rangle$ is defined as ensemble mean over realizations generated by the stochastic forcing, δ is the Delta function, and q^2 is the intensity of the stochastic forcing.

2.2. Prediction Model and Error Variance

Let $\mathbf{y}(t) = [y^{(1)}(t), y^{(2)}(t), \dots, y^{(n)}(t)]$ be the estimate of $\mathbf{x}(t)$ using a prediction model

$$\frac{d\mathbf{y}}{dt} = \mathbf{h}(\mathbf{y}, t) \quad (6a)$$

with an initial condition

$$\mathbf{y}(t_0) = \mathbf{y}_0 \quad (6b)$$

where \mathbf{y}_0 is the initial value of \mathbf{y} .

Difference between reality (\mathbf{x}) and prediction (\mathbf{y}) at any time $t (> t_0)$

$$\mathbf{z} = \mathbf{x} - \mathbf{y}$$

is defined by the prediction error vector and this difference at t_0

$$\mathbf{z}_0 = \mathbf{x}_0 - \mathbf{y}_0$$

is defined by the initial error vector. If the components $[x^{(1)}(t), x^{(2)}(t), \dots, x^{(n)}(t)]$ are not equally important in terms of prediction, the uncertainty of model prediction can be measured by the error variance

$$\text{Var}(\mathbf{z}) = \langle \mathbf{z}^t \mathbf{A} \mathbf{z} \rangle \quad (7)$$

Here, the superscript 't' indicates the transpose of the prediction error vector \mathbf{z} . \mathbf{A} is an $n \times n$ weight matrix.

3. Valid Prediction Period

3.1. Indirect Estimation from IE Growth Rate

Use of IE is to investigate the model error growth due to an initial error,

$$\mathbf{z}(t_0) = \mathbf{z}_0 \quad (8)$$

where t_0 is the initial time. To evaluate model predictability becomes to analyze stability of the system to the given initial analysis error, \mathbf{z}_0 . Thus, many instability theories can be easily incorporated, such as the leading (largest) Lyapunov exponent [e.g., Lorenz 1969] or the amplification factors calculated from the leading singular vectors [e.g., Farrell and Ioannou, 1996 a, b]. Taking a linear time-dependent dynamical system

$$\frac{d\mathbf{x}}{dt} = \mathbf{A}(t)\mathbf{x}, \quad (9)$$

as an example. The first Lyapunov exponent is defined as

$$\lambda = \limsup_{t \rightarrow \infty} \frac{\ln(\|\Phi(t, t_0)\|)}{t} \quad (10)$$

where the propagator $\Phi(t)$ is given by [Coddington and Levinson, 1955]

$$\Phi(t, t_0) = \mathbf{I} + \int_{t_0}^t \mathbf{A}(s) ds + \int_{t_0}^t \mathbf{A}(r) dr \int_{t_0}^r \mathbf{A}(s) ds + \dots$$

where \mathbf{I} is the unit matrix. The only information we can get here is: the larger the value of λ , the shorter the model VPP. Usually, the e-folding scale relating to the IE growth rate is used to represent VPP.

3.2. Direct Calculation

To quantify VPP, we first define two model error limits: minimum (noise level ξ_{noise}) and maximum (tolerance level ε). The model prediction is considered 'accurate' if the model error is less than the noise level,

$$\text{Var}(\mathbf{z}) \leq \xi_{\text{noise}}^2 \quad (11)$$

The model prediction is meaningful only if the error variance is less than tolerance level,

$$\text{Var}(\mathbf{z}) \leq \varepsilon^2 \quad (12)$$

representing an ellipsoid $S_\varepsilon(t)$ with $\mathbf{y}(t)$ as its center (Fig. 1). VPP is represented by a time period $(t - t_0)$ at which \mathbf{z} (the error) first goes out of the ellipsoid $S_\varepsilon(t)$. The parameter $(t - t_0)$ is usually a random variable. The joint probability density function of $(t - t_0)$ and \mathbf{z}_0 satisfies the backward Fokker-Planck equation [Section 3.6 in Gardiner, 1983]

$$\frac{\partial P}{\partial t} - [\mathbf{f}(\mathbf{z}_0, t)] \frac{\partial P}{\partial \mathbf{z}_0} - \frac{1}{2} q^2 \mathbf{z}_0^2 \frac{\partial^2 P}{\partial \mathbf{z}_0 \partial \mathbf{z}_0} = 0.$$

(13)

If the initial error exceeds the tolerance level [i.e., \mathbf{z}_0 hits the boundary of $S_\varepsilon(t_0)$], the model loses prediction capability initially

$$P(t_0, \mathbf{z}_0 \in S_\varepsilon(t_0), 0) = 0. \quad (14)$$

The model also loses prediction capability at $t = \infty$ [Gardiner, 1984]

$$\lim_{t \rightarrow \infty} P(t_0, \mathbf{z}_0, t - t_0) = 0.$$

Temporal integration of $P(t_0, \mathbf{z}_0, t - t_0)$ from t_0 to ∞ should be one,

$$\int_{t_0}^{\infty} P(t_0, \mathbf{z}_0, t - t_0) dt = 1. \quad (15)$$

Since $P(t_0, \mathbf{z}_0, t - t_0)$ is the probability of VPP ($t - t_0$) with the initial error vector \mathbf{z}_0 at t_0 , its first moment

$$\tau_1(\mathbf{z}_0) = \int_{t_0}^{\infty} P(t_0, \mathbf{z}_0, t - t_0) (t - t_0) dt \quad (16)$$

denotes the ensemble mean VPP. Its second moment

$$\tau_2(\mathbf{z}_0) = \int_{t_0}^{\infty} P(t_0, \mathbf{z}_0, t - t_0) (t - t_0)^2 dt$$

(17) indicates the variation of VPP. Both (16) and (17) indicate the dependence of the ensemble mean and variance of VPP on the initial error \mathbf{z}_0 .

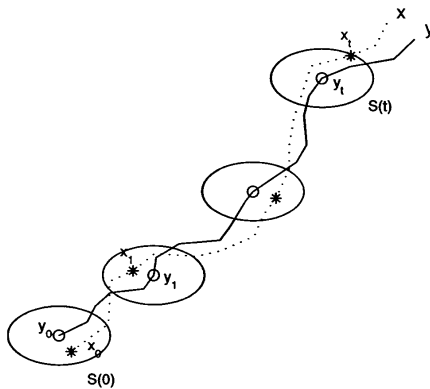


Figure 1. Phase space trajectories of model prediction y (solid curve) and reality x (dashed curve) and error ellipsoid $S_d(t)$ centered at y . The positions of reality and prediction trajectories at time instance are

denoted by “*” and “o”, respectively). A valid prediction is represented by a time period ($t - t_0$) at which the error first goes out of the ellipsoid $S_d(t)$.

3.3. Autonomous Dynamical System

Usually, two steps are used in computing the mean and variance of VPP: (a) to obtain $P(t_0, \mathbf{z}_0, t - t_0)$ after solving the backward Fokker-Planck equation (13), and (b) to compute the mean and variance of VPP using (16) and (17). For an autonomous dynamical system,

$$\mathbf{f} = \mathbf{f}(\mathbf{z}_0)$$

we multiply the backward Fokker-Planck equation (13) is by $(t - t_0)$ and $(t - t_0)^2$, integrated both equations with respect to t from t_0 to ∞ , and obtain the mean VPP equation

$$\mathbf{f}(\mathbf{z}_0) \frac{\partial \tau_1}{\partial \mathbf{z}_0} + \frac{q^2 \mathbf{z}_0^2}{2} \frac{\partial^2 \tau_1}{\partial \mathbf{z}_0 \partial \mathbf{z}_0} = -1 \quad (18)$$

and the VPP variability equation

$$\mathbf{f}(\mathbf{z}_0) \frac{\partial \tau_2}{\partial \mathbf{z}_0} + \frac{q^2 \mathbf{z}_0^2}{2} \frac{\partial^2 \tau_2}{\partial \mathbf{z}_0 \partial \mathbf{z}_0} = -2\tau_1 \quad (19)$$

Both (18) and (19) are linear, time-independent, and second-order differential equations with the initial error \mathbf{z}_0 as the only independent variable. To solve these two equations, two boundary conditions for τ_1 and τ_2 are needed. When the initial error reaches the tolerance level, $\text{Var}(\mathbf{z}_0) = \varepsilon^2$, the model prediction capability is lost no matter how good the model is, and τ_1 and τ_2 become zero,

$$\tau_1 = 0, \tau_2 = 0 \quad \text{for } \text{Var}(\mathbf{z}_0) = \varepsilon^2. \quad (20)$$

When the initial error is below the noise level, ξ_{noise} , the initial condition is considered as ‘accurate’. The model capability of prediction does not depend on the initial condition error (i.e., τ_1 and τ_2 are independent on \mathbf{z}_0),

$$\frac{\partial \tau_1}{\partial \mathbf{z}_0} = 0, \frac{\partial \tau_2}{\partial \mathbf{z}_0} = 0 \quad \text{for } \text{Var}(\mathbf{z}_0) = \xi_{\text{noise}}^2. \quad (21)$$

4. Example

4.1 One-Dimensional Stochastic Dynamical System

We use a one-dimensional probabilistic error growth model [Nicolis, 1992]

$$\frac{d\xi}{dt} = (\sigma\xi - g\xi^2) + v(t)\xi, \quad 0 \leq \xi < \infty \quad (22)$$

as an example to illustrate the process of computing mean VPP and VPP variability. Here, the variable ξ corresponds to the positive Lyapunov exponent σ , g is a non-negative parameter whose properties depend on the underlying attractor, and $v(t)\xi$ is the stochastic forcing satisfying the condition

$$\langle v(t) \rangle = 0, \quad \langle v(t)v(t') \rangle = q^2 \delta(t-t').$$

Without the stochastic forcing, $v(t)\xi$, the model (22) becomes the projection of the Lorenz attractor onto the unstable manifold.

4.2. IE Analysis

The PDF of the random variable ξ in (22), $\hat{P}(\xi, t)$, satisfies the Fokker-Planck equation [Nicolis, 1992]

$$\frac{\partial \hat{P}}{\partial t} + \frac{\partial}{\partial \xi} [(\sigma\xi - g\xi^2)\hat{P}] = \frac{q^2}{2} \frac{\partial^2}{\partial \xi^2} (\xi^2 \hat{P}) \quad (23)$$

Multiplying both sides of (23) by ξ and averaged over $\hat{P}(\xi, t)$ leads to the time evolution of the ensemble mean error

$$\frac{d\langle \xi \rangle}{dt} = \sigma \langle \xi \rangle - g \langle \xi \rangle^2 - g \langle \Delta \xi^2 \rangle \quad (24)$$

where $\langle \Delta \xi^2 \rangle$ is the variance. Both (23) and (24) are used to evaluate model predictability with given initial condition, $\langle \xi \rangle|_{t=0}$, or initial error distribution, $\hat{P}(\xi, 0)$.

For example, Nicolis [1992] investigated the predictability of the stochastic dynamical system (5). With a given initial error distribution

$$\hat{P}(\xi, 0) = \delta(\xi), \quad (25)$$

she integrated the Fokker-Planck equation (23) to obtain the time evolution of $\hat{P}(\xi, t)$.

With a given initial error

$$\langle \xi \rangle|_{t=0} = 1.6 \times 10^{-2} \quad (26)$$

she integrated the nonlinear equation (24) numerically to obtain the time evolution of ensemble mean error $\langle \xi \rangle_t$. The model predictability can be easily evaluated from temporal variability of $\hat{P}(\xi, t)$ and $\langle \xi \rangle_t$.

4.3. Equations for Mean and Variance of VPP

How long is the model (22) valid since being integrated from the initial state?

Or what are the mean and variance of VPP of (22)? To answer these questions, we should first find the equations depicting VPP of (22). Applying the theory described in Sections 3.2 and 3.3 to the model (22), the PDF for the random variable $(t - t_0)$, [i.e., VPP] satisfies the backward Fokker-Planck equation,

$$\frac{\partial P}{\partial t} - [\sigma\xi_0 - g\xi_0^2] \frac{\partial P}{\partial \xi_0} - \frac{1}{2} q^2 \frac{\partial^2 P}{\partial \xi_0^2} = 0 \quad (27)$$

with the initial error (ξ_0) bounded by,

$$\xi_{noise} \leq \xi_0 \leq \varepsilon.$$

Furthermore, equations (18) and (19) become ordinary differential equations

$$(\sigma\xi_0 - g\xi_0^2) \frac{d\tau_1}{d\xi_0} + \frac{q^2 \xi_0^2}{2} \frac{d^2 \tau_1}{d\xi_0^2} = -1 \quad (28)$$

$$(\sigma\xi_0 - g\xi_0^2) \frac{d\tau_2}{d\xi_0} + \frac{q^2 \xi_0^2}{2} \frac{d^2 \tau_2}{d\xi_0^2} = -2\tau_1 \quad (29)$$

with the boundary conditions,

$$\tau_1 = 0, \quad \tau_2 = 0 \text{ for } \xi_0 = \varepsilon. \quad (30)$$

$$\frac{d\tau_1}{d\xi_0} = 0, \quad \frac{d\tau_2}{d\xi_0} = 0 \text{ for } \xi_0 = \xi_{noise}. \quad (31)$$

4.4. Analytical Solutions

Analytical solutions of (28) and (29) with the boundary conditions (30) and (31) are

$$\tau_1(\bar{\xi}_0, \bar{\xi}_{noise}, \varepsilon) = \frac{2}{q^2} \int_{\bar{\xi}_0}^1 y^{-\frac{2\sigma}{q^2}} \exp\left(\frac{2\varepsilon g}{q^2} y\right) \left[\int_{\bar{\xi}_{noise}}^y x^{\frac{2\sigma}{q^2}-2} \exp\left(-\frac{2\varepsilon g}{q^2} x\right) dx \right] dy \quad (32)$$

and

$$\tau_2(\bar{\xi}_0, \bar{\xi}_{noise}, \varepsilon) = \frac{4}{q^2} \int_{\bar{\xi}_0}^1 y^{-\frac{2\sigma}{q^2}} \exp\left(\frac{2\varepsilon g}{q^2} y\right) \left[\int_{\bar{\xi}_{noise}}^y \tau_1(x) x^{\frac{2\sigma}{q^2}-2} \exp\left(-\frac{2\varepsilon g}{q^2} x\right) dx \right] dy \quad (33)$$

where

$$\bar{\xi}_0 = \xi_0 / \varepsilon, \quad \bar{\xi}_{noise} = \xi_{noise} / \varepsilon$$

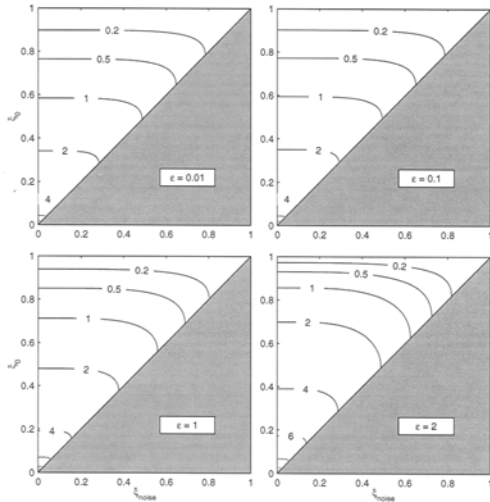
are non-dimensional initial condition error and noise level scaled by the tolerance level ε , respectively. For given tolerance and noise levels (or user input), the mean and

variance of VPP can be calculated using (32) and (33).

4.5. Dependence of τ_1 and τ_2 on $(\bar{\xi}_0, \bar{\xi}_{noise}, \varepsilon)$

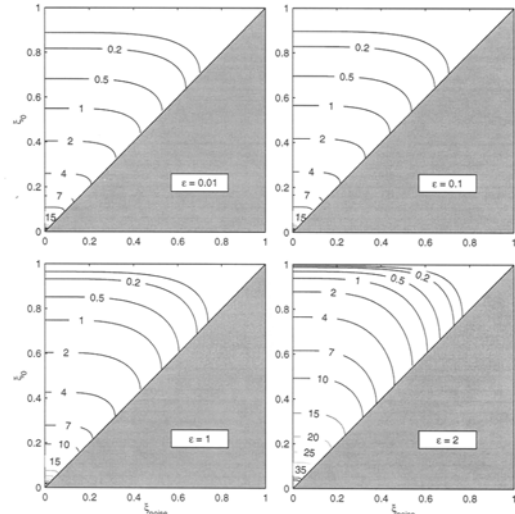
To investigate the sensitivity of τ_1 and τ_2 to $\bar{\xi}_0, \bar{\xi}_{noise}$, and ε , we use the same values for the parameters in the stochastic dynamical system (5) as in *Nicolis* [1992] $\sigma=0.64, g=0.3, q^2=0.2$. (34)

Figures 2 and 3 show the contour plots of $\tau_1(\bar{\xi}_0, \bar{\xi}_{noise}, \varepsilon)$ and $\tau_2(\bar{\xi}_0, \bar{\xi}_{noise}, \varepsilon)$ versus $(\bar{\xi}_0, \bar{\xi}_{noise})$ for four different values of ε (0.01, 0.1, 1, and 2). Following features can be obtained: (a) For given values of $(\bar{\xi}_0, \bar{\xi}_{noise})$ [i.e., the same location in the contour plots], both τ_1 and τ_2 increase with the tolerance level ε . (b) For a given value of tolerance level ε , both τ_1 and τ_2 are almost independent on the noise level $\bar{\xi}_{noise}$ (contours are almost paralleling to the horizontal axis) when the initial error $(\bar{\xi}_0)$ is much larger than the noise level $(\bar{\xi}_{noise})$. This indicates that the effect of the noise level $(\bar{\xi}_{noise})$ on τ_1 and τ_2 becomes evident only when the initial error $(\bar{\xi}_0)$ is close to the noise level $(\bar{\xi}_{noise})$. (c) For given values of $(\varepsilon, \bar{\xi}_{noise})$, both τ_1 and τ_2 decrease with increasing initial error $\bar{\xi}_0$.



Figures 2. Contour plots of $\tau_1(\bar{\xi}_0, \bar{\xi}_{noise}, \varepsilon)$ versus $(\bar{\xi}_0, \bar{\xi}_{noise})$ for four different values of ε (0.01, 0.1, 1, and 2) using *Nicolis* model with stochastic forcing $q^2 = 0.2$. The contour plot covers the half domain due to $\bar{\xi}_0 \geq \bar{\xi}_{noise}$.

Figures 4 and 5 show the curve plots of $\tau_1(\bar{\xi}_0, \bar{\xi}_{noise}, \varepsilon)$ and $\tau_2(\bar{\xi}_0, \bar{\xi}_{noise}, \varepsilon)$ versus $\bar{\xi}_0$ for four different values of tolerance level, ε (0.01, 0.1, 1, and 2) and four different values of random noise $\bar{\xi}_{noise}$ (0.1, 0.2, 0.4, and 0.6). Following features are obtained: (a) τ_1 and τ_2 decrease with increasing $\bar{\xi}_0$, which implies that the higher the initial error, the lower the predictability (or VPP) is; (b) τ_1 and τ_2 decrease with increasing noise level $\bar{\xi}_{noise}$, which implies that the higher the noise level, the lower the predictability (or VPP) is; and (c) τ_1 and τ_2 increase with the increasing ε , which implies that the higher the tolerance level, the longer the VPP is. It is noticed that the results presented in this subsection is for a given value of stochastic forcing ($q^2 = 0.2$) only.

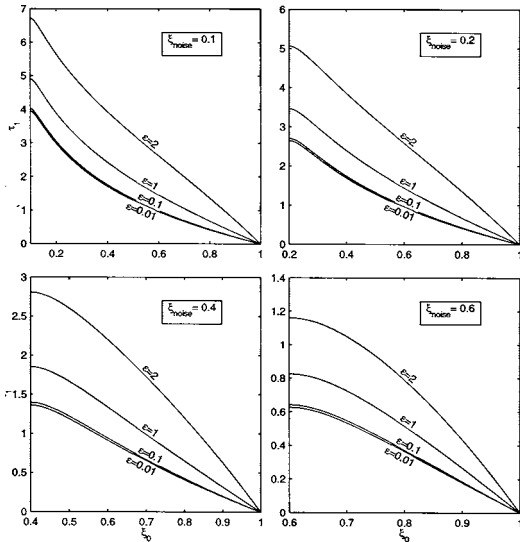


Figures 3. Contour plots of $\tau_2(\bar{\xi}_0, \bar{\xi}_{noise}, \varepsilon)$ versus $(\bar{\xi}_0, \bar{\xi}_{noise})$ for four different values of ε (0.01, 0.1, 1, and 2) using *Nicolis* model with stochastic forcing $q^2 = 0.2$. The contour plot covers the half domain due to $\bar{\xi}_0 \geq \bar{\xi}_{noise}$.

4.6. Dependence of τ_1 and τ_2 on Stochastic Forcing (q^2)

To investigate the sensitivity of τ_1 and τ_2 to the strength of the stochastic forcing, q^2 , we use the same values for the parameters ($\sigma = 0.64$, $g = 0.3$) in (34) as in Nicolis [1992] except q^2 , which takes values of 0.1, 0.2, and 0.4.

Figures 6 and 7 show the curve plots of $\tau_1(\bar{\xi}_0, \bar{\xi}_{noise}, q^2)$ and $\tau_2(\bar{\xi}_0, \bar{\xi}_{noise}, q^2)$ versus $\bar{\xi}_0$ for two tolerance levels ($\varepsilon = 0.1, 1$), two noise levels ($\bar{\xi}_{noise} = 0.1, 0.6$), and three different values of q^2 (0.1, 0.2, and 0.4) representing weak, normal, and strong stochastic forcing. Two regimes are found: (a) τ_1 and τ_2 decrease with increasing q^2 for large noise level ($\bar{\xi}_{noise} = 0.6$), (b) τ_1 and τ_2 increase with increasing q^2 for small noise level ($\bar{\xi}_{noise} = 0.1$), and (c) both relationships (increase and decrease of τ_1 and τ_2 with increasing q^2) are independent on ε . This indicates the existence of stabilizing and destabilizing regimes of the dynamical system depending on stochastic forcing. For a small (large) noise level, the stochastic forcing stabilizes (destabilizes) the dynamical system and extends (shortens) the mean VPP.



Figures 4. Dependence of $\tau_1(\bar{\xi}_0, \bar{\xi}_{noise}, \varepsilon)$ on the initial condition error $\bar{\xi}_0$ for four different values of ε (0.01, 0.1, 1, and 2) and four

different values of random noise $\bar{\xi}_{noise}$ (0.1, 0.2, 0.4, and 0.6) using Nicolis model with stochastic forcing $q^2 = 0.2$.

The two regimes can be identified analytically for small tolerance level ($\varepsilon \rightarrow 0$). The initial error $\bar{\xi}_0$ should also be small ($\bar{\xi}_0 \ll \varepsilon$). The solutions (32) becomes

$$\lim_{\varepsilon \rightarrow 0} \tau_1(\bar{\xi}_0, \bar{\xi}_{noise}, \varepsilon) = \frac{1}{\sigma - q^2/2} \left\{ \ln\left(\frac{1}{\bar{\xi}_0}\right) - \frac{q^2}{2\sigma - q^2} \bar{\xi}_{noise}^{\frac{2\sigma}{q^2} - 1} \left[\left(\frac{1}{\bar{\xi}_0}\right)^{\frac{2\sigma}{q^2} - 1} - 1 \right] \right\} \quad (35)$$

The Lyapunov exponent is identified as $(\sigma - q^2/2)$ for dynamical system (22) [Hasmin'skii 1980]. For a small noise level ($\bar{\xi}_{noise} \ll 1$), the second term in the bracket of the righthand of (35)

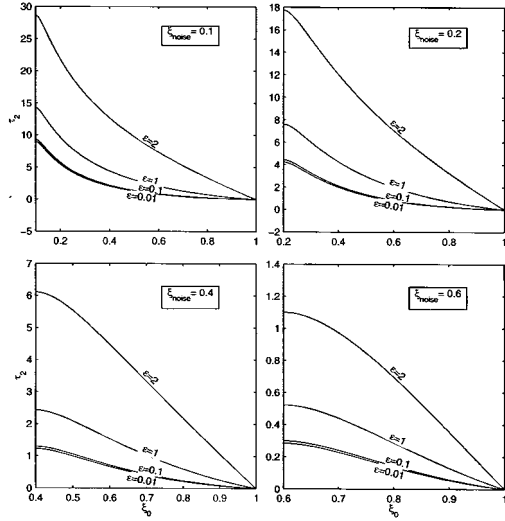
$$R = -\frac{q^2}{2\sigma - q^2} \bar{\xi}_{noise}^{\frac{2\sigma}{q^2} - 1} \left[\left(\frac{1}{\bar{\xi}_0}\right)^{\frac{2\sigma}{q^2} - 1} - 1 \right] \quad (36)$$

is negligible. The solution (35) becomes

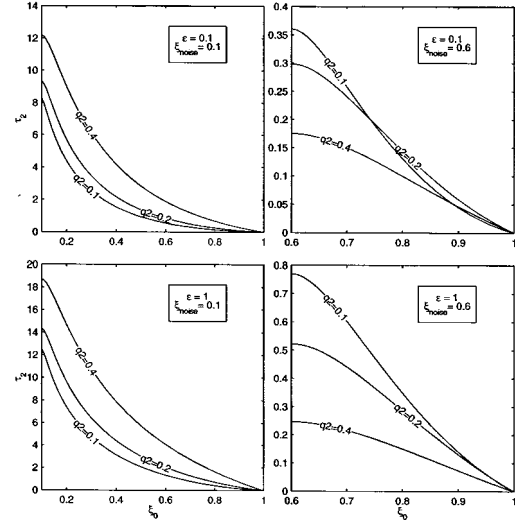
$$\lim_{\varepsilon \rightarrow 0} \tau_1(\bar{\xi}_0, \bar{\xi}_{noise}, \varepsilon) = \frac{1}{\sigma - q^2/2} \ln\left(\frac{1}{\bar{\xi}_0}\right) \quad (37)$$

which shows that the stochastic forcing ($q \neq 0$), reduces the Lyapunov exponent ($\sigma - q^2/2$), stabilizes the dynamical system (22), and in turn increases the mean VPP. On the other hand, the initial error $\bar{\xi}_0$ reduces the mean VPP.

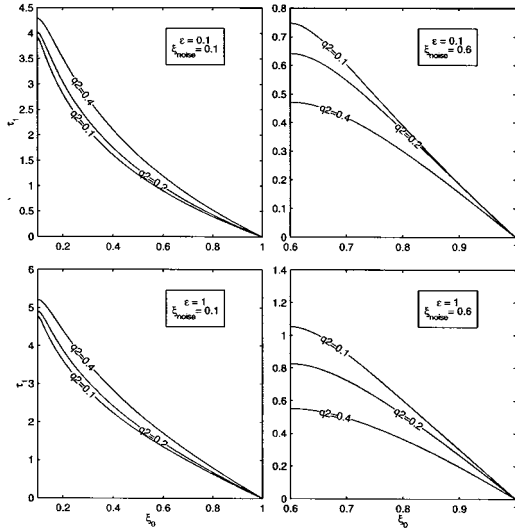
For a large noise level $\bar{\xi}_{noise}$, the second term in the bracket of the righthand of (35) is not negligible. For a positive Lyapunov exponent, $2\sigma - q^2 > 0$, this term is always negative [see (36)]. The absolute value of R increases with increasing q^2 (remember that $\bar{\xi}_{noise} < 1$, $\bar{\xi}_0 < 1$). Thus, the term (R) destabilizes the one-dimensional stochastic dynamical system (22), and reduces the mean VPP.



Figures 5. Dependence of $\tau_2(\bar{\xi}_0, \bar{\xi}_{noise}, \epsilon)$ on the initial condition error $\bar{\xi}_0$ for four different values of ϵ (0.01, 0.1, 1, and 2) and four different values of random noise $\bar{\xi}_{noise}$ (0.1, 0.2, 0.4, and 0.6) using Nicolis model with stochastic forcing $q^2 = 0.2$.



Figures 7. Dependence of $\tau_2(\bar{\xi}_0, \bar{\xi}_{noise}, q^2)$ on the initial condition error $\bar{\xi}_0$ for three different values of the stochastic forcing q^2 (0.1, 0.2, and 0.4) using Nicolis model with Two different values of ϵ (0.1, and 1) and two different values of noise level $\bar{\xi}_{noise}$ (0.1, and 0.6).



Figures 6. Dependence of $\tau_1(\bar{\xi}_0, \bar{\xi}_{noise}, q^2)$ on the initial condition error $\bar{\xi}_0$ for three different values of the stochastic forcing q^2 (0.1, 0.2, and 0.4) using Nicolis model with Two different values of ϵ (0.1, and 1) and two different values of noise level $\bar{\xi}_{noise}$ (0.1, and 0.6).

6. Conclusions

(1) The model valid prediction period ($t - t_0$) depends not only on the instantaneous error growth, but also on the noise level, the tolerance level, and the initial error. A theoretical framework was developed in this study to determine the mean (τ_1) and variability (τ_2) of model valid prediction period for nonlinear stochastic dynamical system. The joint probability density function of the valid prediction period and initial error satisfies the backward Fokker-Planck equation when the valid prediction period is assumed homogeneous. After solving the backward Fokker-Planck equation, it is easy to obtain the ensemble mean and variance of the model valid prediction period.

(2) Uncertainty in ocean (or atmospheric) models are caused by measurement errors (initial and/or boundary condition errors), model discretization, and uncertain model parameters. This leads to the inclusion of stochastic forcing in ocean (atmospheric) models. The backward Fokker-Planck equation can be used for evaluation of ocean (or atmospheric) model predictability through calculating the mean model valid prediction period.

(3) For an autonomous dynamical system, time-independent second-order linear differential equations are derived for τ_1 and τ_2 with given boundary conditions. This is a well-posed problem and the solutions are easily obtained.

(4) For the Nicolis [1992] model, the second-order ordinary differential equations of τ_1 and τ_2 have analytical solutions, which clearly show the following features: (a) decrease of τ_1 and τ_2 with increasing initial condition error (or with increasing random noise), (b) increase of τ_1 and τ_2 with increasing tolerance level ε .

Acknowledgments

This work was supported by the Office of Naval Research (ONR) Naval Ocean Modeling and Prediction (NOMP) Program and the Naval Oceanographic Office. Ivanov wishes to thank the National Research Council (NRC) for the associateship award.

References

- Chu, P.C., 1999: Two kinds of predictability in the Lorenz system. *J. Atmos. Sci.*, **56**, 1427-1432.
- Farrell B.F., and P.J.Ioannou, 1996a: Generalized stability theory. Part 1. Autonomous Operations. *J. Atmos. Sci.*, **53**, 2025-2040.
- Farrell B.F. and P.J.Ioannou, 1996 b: Generalized stability theory Part 2. Nonautonomous Operations. *J. Atmos. Sci.*, **53**, 2041-2053.
- Gardiner C.W., 1985: Handbook of Stochastic Methods for Physics, Chemistry and the Natural Sciences, Springer-Verlag, New York, 526pp.
- Ivanov L.M., A.D.Kirwan, Jr., and O.V.Melnichenko, 1994: Prediction of the stochastic behavior of nonlinear systems by deterministic models as a classical time-passage probabilistic problem. *Nonlinear Proc. Geophys.*, **1**, 224-233.
- Ivanov L.M., T.M. Margolina and O.V.Melnichenko, 1999: Prediction and management of extreme events based on a simple probabilistic model of the first-passage boundary. *Phys. Chem. Earth (A)*, **24**, 169-173.
- Lorenz, E.N., 1963: Deterministic nonperiodic flow. *J. Atmos. Sci.*, **20**, 130-141.
- Lorenz, E.N. , 1969: Atmospheric predictability as revealed by naturally occurring analogues. *J. Atmos. Sci.*, **26**, 636-646.
- Lorenz, E.N. , 1984: Irregularity: A fundamental property of the atmosphere. *Tellus*, **36A**, 98-110.
- Nicolis C., 1992: Probabilistic aspects of error growth in atmospheric dynamics. *Q.J.R. Meteorol. Soc.*, **118**, 553-568.
- Nicolis C., V. Vannitsem and J.-F. Royer, 1995: Short-range predictability of atmosphere: mechanisms for superexponential error growth. *Q.J.R. Meteorol. Soc.*, **121**, 705-722.